Longitudinal Shock Waves in Soil

Vladimir A. Osinov(✉)

Institute of Soil Mechanics and Rock Mechanics, Karlsruhe Institute of Technology, 76128 Karlsruhe, Germany
vladimir.osinov@kit.edu

Abstract. The stiffness of soils in compression increases with increasing pressure. This property makes the strain-stress relation nonlinear and strongly influences the propagation of compression waves: a smooth wave front steepens and turns into a shock front. This paper discusses some theoretical questions related to the formation and propagation of longitudinal shock waves in soil within the pressure range typical of geotechnical engineering problems (up to a few megapascals). In particular, the topics discussed in the paper are the critical distance for dry and saturated soils (the distance covered by a smooth front before it becomes discontinuous), the jump conditions on a discontinuity, and smooth viscous shocks.

1 Introduction

A shock wave in a continuum in a narrow mathematical sense is a discontinuity in the stress and velocity which moves with respect to the medium. In a broader sense, a shock wave is the part of a continuous wave where the stress and velocity change sharply on an interval much smaller than the characteristic length of the problem under study. Shock waves as moving discontinuities can exist in both linearly elastic and nonlinear media. In a linearly elastic medium, a shock wave can be induced by a discontinuous step-like boundary condition, e.g. through an impact or a collision with another body. In a nonlinear medium, a shock front as a moving discontinuity can form even if the boundary condition is continuous. The property of the medium responsible for the shock formation in this case is the increase in the compressional stiffness with increasing pressure. This property is characteristic of the constitutive response of soils.

This paper discusses some theoretical aspects of the formation and propagation of shock waves in soil. Shock waves are often associated not only with high strain rates but also with high pressures produced, for instance, in situ by explosions. Actually, neither the emergence nor the propagation of a shock front require the pressure to be high. The pressure amplitude does play a role for the choice of the constitutive model for the mathematical description of the dynamic deformation and, in particular, a shock wave in the soil. We assume that the pressure does not exceed a few megapascals and thus lies within the range typical of geotechnical engineering problems. We will consider plane longitudinal waves with the simplest deformation mode – uniaxial compression (except

T. Triantafyllidis (Ed.): *Recent Developments of Soil Mechanics and Geotechnics in Theory and Practice*, LNACM 91, pp. 199–217, 2020.
https://doi.org/10.1007/978-3-030-28516-6_11

for some reference made to spherical and cylindrical longitudinal waves as well). The main two issues addressed in the paper are

- the formation of a shock front from a continuous wave and
- the propagation of a shock front.

2 Shock Formation. Plane Waves

We will study plane longitudinal waves propagating along the x_1-axis of a Cartesian coordinate system (x_1, x_2, x_3). The waves have one nonzero velocity component v_1 and three nonzero stress components $\sigma_{11}, \sigma_{22}, \sigma_{33}$. In what follows, we will write for brevity x for x_1, v for v_1 and σ for σ_{11}. The stress components σ_{22}, σ_{33} will not be considered. The governing equations will be written in the small-strain approximation with the partial time derivatives instead of the material ones. The density of the medium will be treated as a constant. Compressive stresses and deformations are taken to be negative according to the sign convention of continuum mechanics.

The equation of motion for the waves reads

$$\frac{\partial \sigma}{\partial x} = \varrho \frac{\partial v}{\partial t}, \tag{1}$$

where ϱ is the density and t is the time variable. For rate-independent behaviour, the constitutive equation can be written in rate form as

$$\frac{\partial \sigma}{\partial t} = k \frac{\partial \varepsilon}{\partial t}, \tag{2}$$

where ε is the axial deformation and k is the stiffness. Using the kinematic relation

$$\frac{\partial \varepsilon}{\partial t} = \frac{\partial v}{\partial x}, \tag{3}$$

the constitutive equation can be written as

$$\frac{\partial \sigma}{\partial t} = k \frac{\partial v}{\partial x}. \tag{4}$$

The wave propagation is described by the hyperbolic system of two Eqs. (1), (4) for two unknown functions $v(x,t), \sigma(x,t)$. The system has two families of characteristics with the slopes $dt/dx = \pm\sqrt{\varrho/k}$.

Consider a half-space $x \geq 0$ with a homogeneous initial stress σ^+ and zero initial velocity. Let a stress $\sigma_b(t)$ with $\sigma_b(0) = \sigma^+$ be applied at the boundary $x = 0$. This stress induces a wave propagating in the half space. If the medium is linearly elastic with $k = \text{const}$, the system (1), (4) is linear, and we obtain a travelling-wave solution: the wave propagates with the characteristic wave speed $c = \sqrt{k/\varrho}$ without changing its shape. Let σ^+ be equal to $-100\,\text{kPa}$ and $\sigma_b(t)$ represent an increasing compressive stress as shown in Fig. 1. The travelling wave induced by this boundary condition is shown in Fig. 2 for $c = 400\,\text{m/s}$.

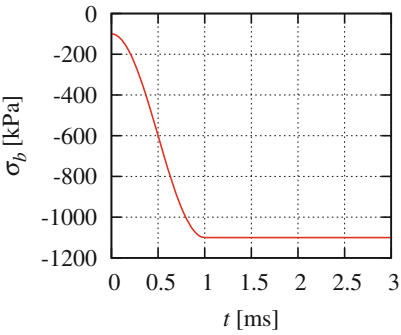

Fig. 1. Boundary condition at $x = 0$ for the solutions in Figs. 2 and 3

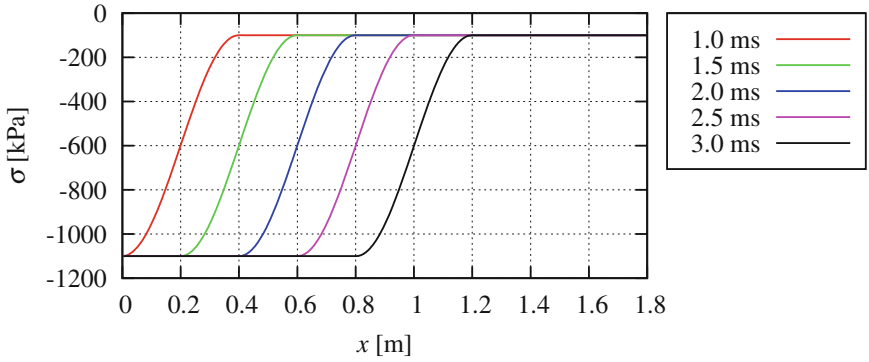

Fig. 2. Wave profiles in the half-space $x \geq 0$ at different times for constant stiffness k with the boundary condition in Fig. 1

The situation becomes qualitatively different if the wave propagates, for instance, in a dry granular soil and the stress increase is sufficiently large, like in the present example. The uniaxial (oedometric) compression of the soil up to a few megapascals yields a nonlinear strain-stress relation $\sigma(\varepsilon)$ with the increasing stiffness $k = d\sigma/d\varepsilon$ (higher pressures will not be considered here, as they may change the shape of the strain-stress curve because of grain crushing). For a given curve $\sigma(\varepsilon)$ obtained for the compression, k may be thought of as a function of either ε or σ. Writing $k(\sigma)$ allows us to consider again the system (1), (4) for the same unknown functions v, σ. However, the system becomes quasilinear: the coefficient k depends on the solution σ.

An important question is whether the quasilinear system with the stress-dependent stiffness $k(\sigma)$ possesses travelling-wave solutions like the linear system. Let $\sigma(\xi), v(\xi)$ be such a solution, where $\xi = t - x/c$, and c is the speed of propagation. The partial derivatives of the functions $\sigma(\xi), v(\xi)$ satisfy the equalities

$$\frac{\partial \sigma}{\partial t} + c\,\frac{\partial \sigma}{\partial x} = 0, \quad \frac{\partial v}{\partial t} + c\,\frac{\partial v}{\partial x} = 0. \tag{5}$$

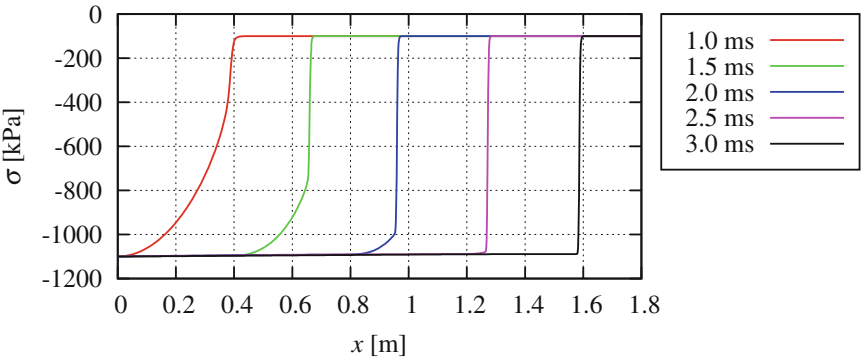

Fig. 3. Wave profiles in the half-space $x \geq 0$ at different times for the stress-dependent stiffness $k(\sigma)$ given by (16)

Let us calculate the stiffness of a material element using this solution. Beginning with the definition of k and then taking into account (5), the kinematic relation (3), the equation of motion (1) and again (5), we obtain

$$k = \frac{\partial \sigma}{\partial t}\left(\frac{\partial \varepsilon}{\partial t}\right)^{-1} = -c\,\frac{\partial \sigma}{\partial x}\left(\frac{\partial v}{\partial x}\right)^{-1} = \varrho c^2\,\frac{\partial v}{\partial t}\left(\frac{\partial v}{\partial t}\right)^{-1} = \varrho c^2. \tag{6}$$

This shows that, because c is a constant, k must be a constant as well. Thus, for travelling-wave solutions to exist, the strain-stress relation $\sigma(\varepsilon)$ must be linear.

For a nonlinear strain-stress relation such as in dry soil, two neighbouring points on a moving wave profile propagate with different wave speeds: the point with a higher stress moves faster than the point with a lower stress. For the boundary condition with the increasing compressive stress shown in Fig. 1, the wave profile steepens during the propagation until the gradients $\partial\sigma/\partial x$, $\partial v/\partial x$ become infinite at some point of the profile. At that instant, a discontinuity in the solution (a shock) arises, and the solution differentiable everywhere in the domain does not exist any longer. Figure 3 shows the numerical solution for the same boundary loading as in Fig. 1 with a nonlinear constitutive function $\sigma(\varepsilon)$ for dry soil. The constitutive function and the method of solution will be discussed below in Sects. 4 and 5. Here the focus is on the fact that the continuous front turns into a shock at a distance of about 0.5 m from the boundary.

The mechanism of the transition from a continuous compression front to a shock is well known and is in essence the same for fluids and solids [1–5]. It is also a general property of quasi-linear systems that the solution may become discontinuous in a finite time even if the initial and boundary data are continuous [6]. The time at which the solution loses continuity is called the critical time. In the case of the boundary value problem for the half-space formulated above, the coordinate x at which the gradients $\partial\sigma/\partial x$, $\partial v/\partial x$ become infinite at the critical time is called the critical distance.

The solution to the boundary value problem for the half-space with stress-dependent stiffness is continuous up to the critical time. This solution is a

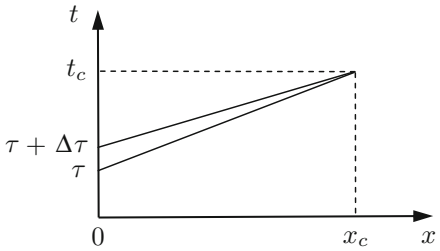

Fig. 4. Two straight characteristics on the (x, t)-plane

so-called simple wave [1]: the characteristics with the positive slopes $dt/dx = \sqrt{\varrho/k(\sigma_b)}$ emanating from the t-axis on the (x, t)-plane are straight lines, and the functions σ, v are constant on these characteristics, Fig. 4. The values of v on the t-axis, $v_b(t) = v(0, t)$, are found from the solution of the ordinary differential equation

$$\frac{dv_b}{dt} = -\frac{1}{\sqrt{\varrho k(\sigma_b)}} \frac{d\sigma_b}{dt} \tag{7}$$

with $v_b(0) = 0$ (the initial condition for v). It can be verified directly that this simple-wave solution satisfies the system (1), (4). For details and for a more general system of two quasilinear equations, see [7].

The simple-wave solution allows us to derive an ordinary differential equation for a certain linear combination of the gradients $\partial\sigma/\partial x$, $\partial v/\partial x$ as functions of x along a given characteristic with a positive slope [7]. The differential equation obtained is of the Bernoulli type. The equation has the property that the solution may become infinite at a finite value of the independent variable. The equation can be integrated to find the coordinate x at which the gradients tend to infinity. This coordinate may be interpreted as the critical distance for a particular characteristic and will be denoted by $x_c(\tau)$, where τ is the time at which the characteristic emanates from the t-axis, see Fig. 4.

If the knowledge of the gradients along the characteristic is not needed, the value of $x_c(\tau)$ alone can be found in a simpler way. Consider two neighbouring characteristics with positive slopes emanating from the t-axis at times τ and $\tau + \Delta\tau$ as shown in Fig. 4. For the increasing stress at the boundary shown in Fig. 1, the slope dt/dx of the characteristic for τ with $\sigma_b(\tau)$ will be greater than the slope of the characteristic for $\tau + \Delta\tau$ with $\sigma_b(\tau + \Delta\tau)$, because the latter corresponds to a higher stiffness and a higher wave speed. The two characteristics cross at some x giving two different values of σ at this x, and the same is true for v (recall that σ and v are constant on these characteristics in the simple-wave solution). The solution must therefore be discontinuous at this point. If $\Delta\tau \to 0$, the intersection point tends to a point which gives the critical distance $x_c(\tau)$ for this characteristic. The gradients $\partial\sigma/\partial x$, $\partial v/\partial x$ become infinite at $x_c(\tau)$. The two characteristics in Fig. 4 are described on the (x, t)-plane by the equations

$$t = \frac{x}{c(\tau)} + \tau, \quad t = \frac{x}{c(\tau + \Delta\tau)} + \tau + \Delta\tau, \tag{8}$$

where $c(\tau) = \sqrt{k(\sigma_b(\tau))/\varrho}$ is the wave speed as a function of τ. If $\Delta\tau \to 0$, the two lines (8) cross at

$$x_c(\tau) = \lim_{\Delta\tau \to 0} \frac{c(\tau)\, c(\tau + \Delta\tau)\, \Delta\tau}{c(\tau + \Delta\tau) - c(\tau)} = c^2 \left(\frac{dc}{d\tau}\right)^{-1}. \tag{9}$$

This is the same $x_c(\tau)$ as the one that would be obtained from the solution to the Bernoulli equation mentioned above.

The time $t_c(\tau)$ at which the gradients become infinite at $x_c(\tau)$ is

$$t_c(\tau) = \tau + \frac{x_c(\tau)}{c(\tau)}. \tag{10}$$

The critical time for the boundary value problem, denoted by $\hat{t}_c$, is therefore

$$\hat{t}_c = \min_{\tau} t_c(\tau). \tag{11}$$

The critical distance $\hat{x}_c$, defined above as the coordinate at which the gradients become infinite at the critical time, is given by

$$\hat{x}_c = x_c(\hat{\tau}), \tag{12}$$

where $\hat{\tau}$ satisfies the equation $\hat{t}_c = t_c(\hat{\tau})$.

Finding the critical distance $\hat{x}_c$ with (9)–(12) for a particular problem may be a rather intricate procedure. Theoretically, $\hat{x}_c$ may even be nonunique: the gradients may become infinite simultaneously at two different points of the wave profile. In applications, where the strain-stress relation $\sigma(\varepsilon)$ and the boundary condition $\sigma_b(t)$ are known only approximately, it suffices to obtain an estimation of the critical distance from (9) rather than the exact value determined by (12).

Using the definition of c, (9) can be written as

$$x_c(\tau) = \frac{2\,k^{3/2}}{\sqrt{\varrho}} \left(\frac{dk}{d\sigma}\right)^{-1} \left(\frac{d\sigma_b}{d\tau}\right)^{-1} = \frac{2\,k^{5/2}}{\sqrt{\varrho}} \left(\frac{dk}{d\varepsilon}\right)^{-1} \left(\frac{d\sigma_b}{d\tau}\right)^{-1}, \tag{13}$$

where $k, dk/d\sigma, dk/d\varepsilon$ represent the values at the boundary and are functions of τ due to their dependence on $\sigma_b(\tau)$. Let us take a closer look at these expressions for x_c. Since compressive stresses and deformations are taken to be negative, $dk/d\sigma$ and $dk/d\varepsilon$ are negative. For x_c to be positive, the stress rate $d\sigma_b/d\tau$ at the boundary must be negative, that is, the boundary condition must induce a compression front. In the case of an expansion front, formula (13) gives a negative value of x_c. Such a front flattens out as it propagates and does not turn into a shock. For a given strain-stress relation $\sigma(\varepsilon)$, the critical distance is inversely proportional to the stress rate $d\sigma_b/d\tau$: the higher the rate, the shorter x_c. The critical distance is also inversely proportional to the second derivative of the function $\sigma(\varepsilon)$. If $k = \text{const}$, x_c is infinite in accordance with the fact that the wave profile in a linearly elastic medium does not change during the propagation. The critical distance increases with increasing k if all other terms are fixed.

3 Shock Formation. Cylindrical and Spherical Waves

A different way to study the formation of shocks from continuous solutions is to consider acceleration waves, i.e. discontinuities in the first partial derivatives of the functions $\sigma(x,t), v(x,t)$ (called weak discontinuities, as distinct from strong discontinuities, or shocks, when the functions σ, v themselves are discontinuous). This approach is used in [8,9].

A weak discontinuity turns into a shock when the gradients $\partial\sigma/\partial x$, $\partial v/\partial x$ become infinite on one side of the discontinuity. The curve on the (x,t)-plane where the partial derivatives are discontinuous is a characteristic curve of the system. The vector of the jumps, $([\![\partial\sigma/\partial x]\!], [\![\partial v/\partial x]\!])$, is proportional to an eigenvector of the matrix of the system, with the factor being defined as the amplitude of the discontinuity. The amplitude as a function of the distance covered by the front satisfies an ordinary differential equation of the Bernoulli type. The equation can be integrated if the front propagates into a quiescent region with a known stress σ. The coordinate at which the amplitude becomes infinite is the critical distance. As is readily seen from this description, the acceleration-wave method requires the boundary condition $\sigma_b(t)$ to have a nonzero rate $d\sigma_b/dt$ at $t = 0$ for which the critical distance is calculated. The point where infinite gradients arise is the leading point of the wave profile. Although the formula obtained for the critical distance coincides with (13), the method cannot be directly applied to other points of the wave profile.

An advantage of the acceleration-wave method over the previous one is that it is applicable to cylindrical and spherical waves. The equations for such waves include the circumferential stress as an additional unknown function. The equation of motion contains additional terms without derivatives. Continuous cylindrical and spherical waves can turn into shocks as well as plane waves if the stiffness of the medium is stress-dependent. The critical distance is understood as the distance from the cavity wall where the wave is generated by a radial stress $\sigma_b(t)$ applied to the wall. If the constitutive response of the medium satisfies certain isotropy conditions, both plane and cylindrical, or both plane and spherical, waves can exist. In this case, given a loading rate $d\sigma_b/dt$ at the boundary, a question arises as to how the critical distances for the three types of waves differ from each other. As shown in [8], unique relations exist between the critical distances independently of the particular choice of the constitutive function. The relations are also valid for a saturated porous solid in which the pore fluid bulk modulus is a function of the pore pressure.

Let l_P, l_C, l_S be the critical distances calculated with the acceleration-wave method for plane, cylindrical and spherical fronts, respectively. The values of l_C and l_S are connected with l_P by the relations

$$l_C = l_P \left(1 + \frac{l_P}{4r_0}\right), \tag{14}$$

$$l_S = r_0 \left[\exp\left(\frac{l_P}{r_0}\right) - 1\right], \tag{15}$$

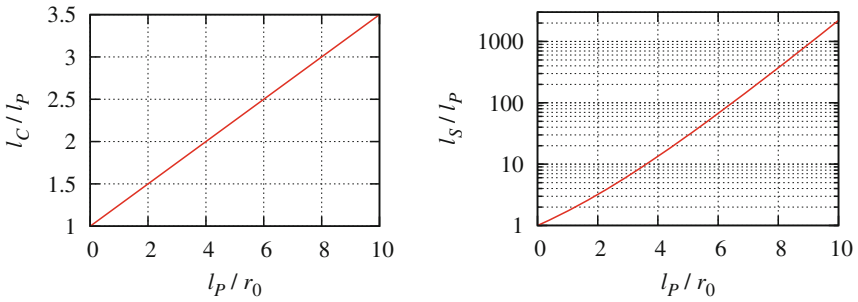

Fig. 5. Relations between the critical distances for plane, cylindrical and spherical fronts [8]

where r_0 is the cavity radius in the cylindrical and spherical problems [8]. It is convenient to plot the ratios l_C/l_P and l_S/l_P as functions of l_P/r_0. These functions are shown in Fig. 5. The distances l_C and l_S are always greater than l_P. If l_P is much smaller than r_0, both l_C and l_S are close to l_P. The growth of l_S/l_P with increasing ratio l_P/r_0 is much faster than that of l_C/l_P.

4 Critical Distances in Soil

In dry granular soils such as sand, the stiffness as a function of the confining pressure is known to obey a power law with an exponent of about 0.5–0.6 [10]. Based on this fact, we consider a simple constitutive model in which the stiffness k for uniaxial deformation is a function of σ of the form

$$k(\sigma) = k_0 \left(\frac{\sigma}{\sigma_0} \right)^m , \tag{16}$$

where k_0 is the value of k at $\sigma = \sigma_0$, and m is a constant. It may be convenient to use, instead of k_0, the wave speed $c_0 = \sqrt{k_0/\varrho}$ in the dry soil at $\sigma = \sigma_0$, where $\varrho = (1-n)\varrho_s$ is the soil density, ϱ_s is the density of the solid phase (grains), and n is the porosity. The strain-stress relation $\sigma(\varepsilon)$ obtained with (16) is shown in Fig. 6 (the curve for $S_r = 0$) with the model parameters given in Table 1.

Table 1. Model parameters

c_0 [m/s]	σ_0 [kPa]	m	n	ϱ_s [kg/m^3]	ϱ_f [kg/m^3]
400	−100	0.6	0.375	2650	1000

Figure 7 shows the critical distance in dry soil as a function of σ calculated with (13), (16) for the boundary rate $d\sigma_b/dt$ equal to -10^3 MPa/s. The boundary loading shown in Fig. 1 would have this rate if the stress increase were linear in

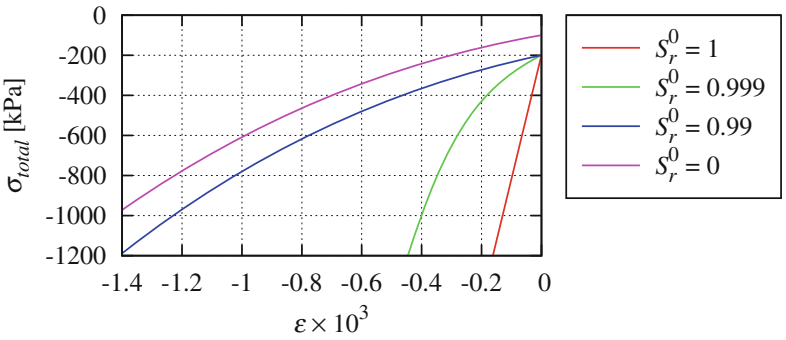

Fig. 6. Strain-stress relations for dry and saturated soils obtained with (16) for an initial effective stress of -100 kPa and, if $S_r \neq 0$, for an initial pore pressure of 100 kPa

time. Since the critical distance is inversely proportional to the stress rate, the values for other rates can easily be found by multiplication. The shock formation observed in Fig. 3 is in good agreement with Fig. 7.

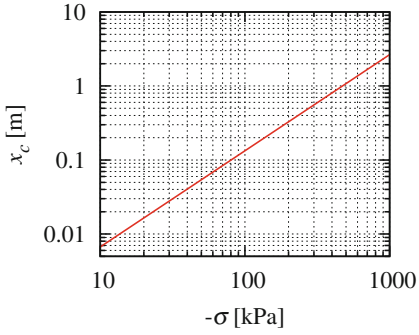

Fig. 7. Critical distance in dry soil as a function of the stress for the boundary rate $d\sigma_b/dt = -10^3$ MPa/s

Formula (13) for the critical distance is applicable to saturated soil if the soil permeability is low enough to assume locally undrained conditions (for nonzero permeability, see [9]). For saturated soil, the stress σ with the stiffness (16) is the effective stress defined as

$$\sigma = \sigma_{total} + p, \tag{17}$$

where σ_{total} is the total stress, and p is the pore pressure (positive for compression). The effective stress σ in (17) is determined by the deformation of the

skeleton if the compressibility of the skeleton is much higher than the compressibility of the solid phase (grains). The equation of motion (1) and the constitutive equation (4) for saturated soil are written as

$$\frac{\partial \sigma_{total}}{\partial x} = \varrho \frac{\partial v}{\partial t}, \tag{18}$$

$$\frac{\partial \sigma_{total}}{\partial t} = \left(k + \frac{K_f}{n} \right) \frac{\partial v}{\partial x}, \tag{19}$$

where $\varrho = (1-n)\varrho_s + n\varrho_f$ is the soil density, ϱ_s, ϱ_f are the densities of the solid and fluid phases, and K_f is the bulk modulus of the pore fluid. The boundary loading $\sigma_b(t)$ is understood as the total stress. The stiffness k in Eq. (13) for the critical distance should be replaced with the total stiffness $k + K_f/n$. Since the compression of saturated soil from a given initial state yields a definite strain-stress function $\sigma_{total}(\varepsilon)$, the total stiffness can be viewed as a function of either the total stress or the skeleton deformation.

Suppose that the pore water contains a small amount (a few volume percent) of free gas. The bulk modulus of such a water-gas mixture, considered as a single fluid, is [11–13]

$$K_f = \left(\frac{S_r}{K_w} + \frac{1 - S_r}{K_g} \right)^{-1}, \tag{20}$$

where S_r is the degree of saturation, K_w is the bulk modulus of pure water (2.2 GPa), and K_g is the bulk modulus of the free gas. The difference between the pressures in the water and in the gas is the capillary pressure due to surface tension at the water-gas interface. For fine sand and high saturation, the pressure difference does not exceed a few kilopascals and is neglected. Furthermore, the mass of the free gas in the pore water is assumed to remain constant (this may not be true for slow compression, as part of the free gas would be dissolved in the water according to the Henry law). For an ideal gas, the bulk modulus K_g is proportional to the absolute gas pressure: $K_g = \gamma(p + p_a)$, where p_a is the atmospheric pressure (100 kPa), $\gamma = 1$ for isothermal processes and $\gamma = 1.4$ for adiabatic processes for air. We take $\gamma = 1$ assuming that the pore water hinders the temperature rise in the gas. For a given degree of saturation S_r^0 at an initial pore pressure p^0, the modulus K_f is a function of the current pressure p [13].

The strain-stress relation for saturated soil is shown in Fig. 6 for three values of S_r^0. If the soil is fully saturated, the pore fluid bulk modulus, K_f, is equal to the modulus of pure water, K_w. Since this modulus is much higher than the skeleton stiffness, the strain-stress relation for the total stress is practically linear. The presence of a small amount of free gas in the pore water substantially reduces the bulk modulus of the pore fluid. As follows from (20), one volume percent of free gas at $p^0 = 100$ kPa reduces K_f from 2.2 GPa to 20 MPa. This makes the soil stiffness nearly the same as in the dry soil, see the curves for $S_r^0 = 0.99$ and $S_r^0 = 0$ in Fig. 6. Even the case with $S_r^0 = 0.999$ is markedly different from full saturation in that the strain-stress relation is nonlinear.

The nonlinearity of the strain-stress relation leads to the formation of shocks for compression fronts. Figure 8 shows the critical distance in saturated soil as a

function of the gas content $1 - S_r$ for the boundary rate $d\sigma_b/dt = -10^3$ MPa/s. Comparison of Figs. 8 and 7 shows that the critical distance in saturated soil is close to that in dry soil for the degrees of saturation up to 0.999. A similar plot with slightly different constitutive parameters can be found in [8].

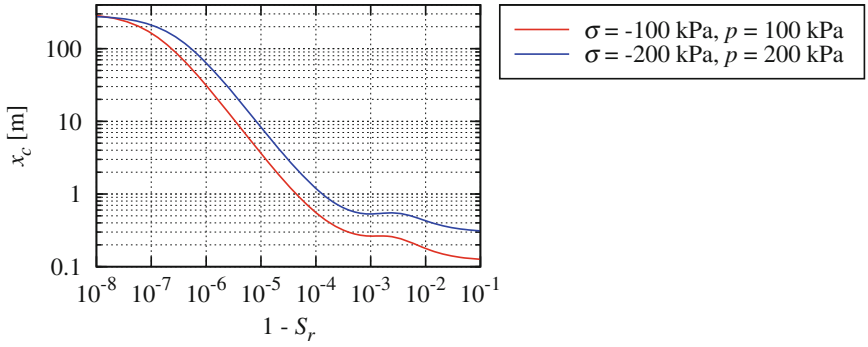

Fig. 8. Critical distance in saturated soil as a function of the gas content for the boundary rate $d\sigma_b/dt = -10^3$ MPa/s

So far we have considered a specific boundary value problem for the half-space with a compressive boundary condition. Of course, if the boundary condition is not compressive but the dynamic process develops in such a way that the soil undergoes compression, shock fronts may also arise. We have seen that the critical distance for fully saturated soil is much larger than in the other cases considered because of the dominant contribution of the bulk modulus of water to the total stiffness of the soil. The constant modulus of water makes the soil stiffness nearly constant as well. However, under certain conditions shock fronts can also arise very quickly in problems with fully saturated soil. If the soil is subjected to tensile deformation, the pore pressure may become sufficiently low to give rise to pore water cavitation. At that instant, the pore fluid bulk modulus abruptly falls from 2.2 GPa to a nearly zero value determined by the compressibility of the vapour in the bubbles. Assuming that the cavitation begins at zero absolute pore pressure and neglecting the vapour pressure, the tensile deformation of the soil produces a strain-stress relation like that shown in Fig. 9. The kink on the curves corresponds to the beginning of cavitation, after which the pore fluid bulk modulus is zero and the soil stiffness is determined solely by the stiffness of the skeleton. As the soil is compressed after the expansion, the strain-stress path will be slightly different from that shown in Fig. 9 due to the plastic behaviour of the skeleton, but the curve will also have a kink at the point where all cavitation bubbles disappear and the fluid bulk modulus is restored to 2.2 GPa. Because of the sharp increase in the stiffness, the compression will produce a shock front. The jump in the stiffness in this simple cavitation model means an infinite second derivative $d^2\sigma_{total}/d\varepsilon^2$ and, as seen from (13), a zero critical distance.

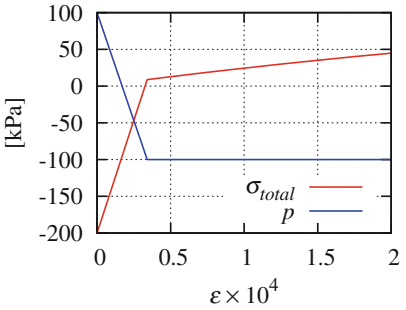

Fig. 9. Strain-stress relation for the expansion of fully saturated soil with the stiffness (16) and the pore water cavitation

Pore water cavitation in fully saturated soil may occur if a large-amplitude pressure wave propagates upwards in the ground and is reflected from the free surface. Examples of such waves induced by an explosion in a tunnel can be found in [14,15]. If the ground were elastic, the reflected wave would have a tensile stress of the same magnitude as the incident wave. In fully saturated soil, large tensile stresses are impossible because neither the skeleton nor the pore water can withstand such stresses. As a result of the interaction of the incident wave with the free surface, a large cavitation zone forms in the soil [14,15]. The subsequent shrinkage of the cavitation zone is accompanied by the formation of shock fronts at the boundary of the cavitation zone according to the mechanism described above. Although the amplitudes of these shock fronts are much smaller than the amplitude of the primary pressure wave, these shocks, like any others, entail numerical problems because of spurious numerical oscillations which are difficult to eliminate.

5 Shock Propagation

After a shock front has formed from the continuous wave, the dynamic deformation can no longer be described by differential equations in the whole domain as before the shock formation. The differential equations cannot be applied directly to a point where the solution is discontinuous. We can still use the differential equations for the smooth part of the wave, but need new relations on the shock to be able to solve the problem further. In this Section we discuss the question of how plane longitudinal shock fronts can be described in the context of soil mechanics and to what extent the description is correct.

Relations on discontinuities can be derived if the dynamic process is governed by differential equations in the form of conservation laws

$$\frac{\partial u_i}{\partial t} + \frac{\partial}{\partial x} f_i(u_1, \ldots, u_N) = 0, \quad i = 1, \ldots, N, \tag{21}$$

where u_i are the unknown functions, and f_i are sufficiently smooth functions of $u_1, \ldots, u_N$. System (21) can be integrated with respect to x and written as

$$\frac{d}{dt}\int_{x_a}^{x_b} u_i dx + f_i(u_1, \ldots, u_N)\Big|_{x_a}^{x_b} = 0, \quad i = 1, \ldots, N, \tag{22}$$

where x_a, x_b are two fixed points. As distinct from (21), the integral form (22) is applicable to discontinuous solutions. Let $[\![u_i]\!] = u_i^+ - u_i^-$ denote the jump in the function u_i across the shock, where u_i^+ and u_i^- are the values ahead of and behind the shock, respectively, as shown in Fig. 10. If the solution has a discontinuity moving with a speed s, the values of the functions on the shock satisfy the Rankine-Hugoniot jump conditions [2–5, 16–18]

$$[\![u_i]\!]s = [\![f_i]\!], \quad i = 1, ..., N. \tag{23}$$

Conditions (23) are obtained by considering a discontinuity between x_a and x_b in (22) and taking the limit $x_b \to x_a$.

We restrict ourselves to plane longitudinal waves in the half-space described by Eqs. (1) and (4) for two unknown functions σ, v, with a monotonic boundary condition like that shown in Fig. 1. To see how many jump conditions are necessary to solve the problem with a shock, consider large times at which the wave consists of the shock and two spatially homogeneous states ahead of and behind the shock, see Fig. 3, $t = 3$ ms and Fig. 10 left. The known quantities are σ^+, v^+ (the initial conditions in the half-space) and σ^- (the boundary condition). The unknown quantities are the velocity v^- behind the shock and the shock speed s. Hence, we need two equations to determine the two unknowns. It can be shown that, if the smooth part of the wave is not homogeneous (Fig. 10 right), we also need two jump conditions to solve the problem in the whole domain.

Whereas Eq. (1) is in the conservation-law form (21) (we assumed $\varrho = \text{const}$), Eq. (4) with variable k is not in this form and does not give any jump condition, unless the medium is linearly elastic with $k = \text{const}$. A second jump condition can be found if we take ε and v as unknown functions and use Eq. (3) instead of (4). The stress σ in (1) is then viewed as a known function of ε obtained from the strain-stress relation for the uniaxial compression. The two Eqs. (1) and (3) give two required jump conditions

$$[\![v]\!]\varrho s = -[\![\sigma]\!], \quad [\![\varepsilon]\!]s = -[\![v]\!]. \tag{24}$$

As follows from (24), the shock speed s is determined by the jumps in the strain and stress as

$$s^2 = \frac{[\![\sigma]\!]}{[\![\varepsilon]\!]\varrho}. \tag{25}$$

A question that arises in connection with the shock description is whether σ^- as a function of ε immediately behind the shock can be obtained from the same strain-stress curve $\sigma(\varepsilon)$ as for the smooth part of the solution. These two functions need not be the same. Moreover, certain considerations suggest that they are different. The difference is due to the way that the soil deforms in time

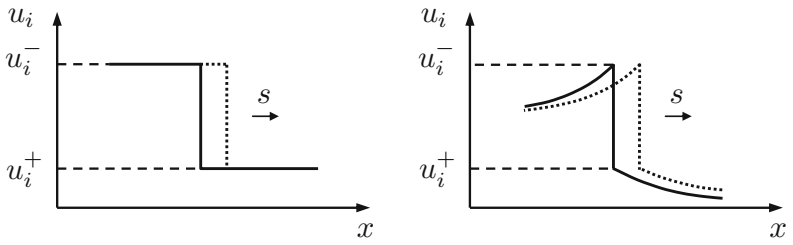

Fig. 10. A propagating shock with homogeneous (left) and inhomogeneous (right) states in the neighbourhood of the shock

and space. Constitutive models of soil mechanics and their calibration are based on the results of element tests (in the present case – the oedometric test). Shock front as a discontinuity in the solution is a mathematical notion pertinent to hyperbolic conservation laws. A real shock front in the soil is continuous with a nonzero thickness which may be assumed not to exceed the size of the soil sample in an element test. The strain rate in an element test is much lower than the strain rate on a shock front. Since the strain rate is equal to the velocity gradient, it tends to infinity as the shock thickness tends to zero. Another essential difference lies in the strain rate gradient. The deformation in an element test is more or less homogeneous, at least for small strains. Although the residual deformation behind a shock can also be spatially homogeneous, the strain rate during the shock passage is inherently inhomogeneous. The smaller the shock thickness, the higher the degree of inhomogeneity in the strain rate. This is illustrated in Fig. 11 for a smooth shock front of thickness Δx. The strain rate in a soil layer of the same thickness Δx is always inhomogeneous, unless it is zero before and after the shock passage. The deformation like that shown in Fig. 11 cannot be reproduced in element tests. More sophisticated dynamic experiments with propagating shocks and inhomogeneous strain rates are required. A high strain rate alone does not suffice. Taking the function $\sigma(\varepsilon)$ for the shock description is an approximation with as yet unknown inaccuracy.

If we accept the necessity of two different functions $\sigma(\varepsilon)$ and $\sigma^-(\varepsilon)$, the overall mathematical description of the dynamic deformation will become more complicated. This concerns, in particular, the analysis of the shock existence and the task of incorporating the two functions into a single boundary value problem.

If the shocks and the continuous deformation are described by the same function $\sigma(\varepsilon)$, one can establish an inequality relation between the shock speed and the characteristic wave speeds ahead of and behind the shock. Assume the function $\sigma(\varepsilon)$ to be such that $d^2\sigma/d\varepsilon^2 < 0$. Since the shocks are compressive, we have $\sigma^+ > \sigma^-$, and it is easy to see that the shock speed given by (25) is greater than the characteristic wave speed $\sqrt{k(\sigma^+)/\varrho}$ ahead of the shock, and less than the characteristic wave speed $\sqrt{k(\sigma^-)/\varrho}$ behind the shock. This result constitutes a necessary condition for the existence of the shock [2–5, 16–18] and is

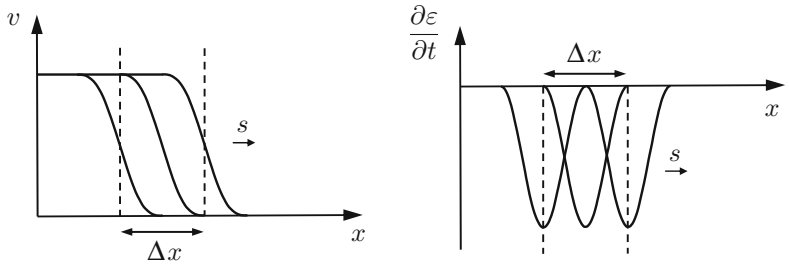

Fig. 11. Velocity and strain rate profiles at different times

also well known from gas dynamics: a shock propagates with a supersonic speed with respect to the medium ahead of the shock, and with a subsonic speed with respect to the medium behind the shock [1].

A better insight into the shock propagation phenomenon can be gained if we try to find the strain-stress path that a soil element follows between ε^+ and ε^- as the shock crosses the element. Note that we could say that it has no sense to speak of a strain-stress path as such, but only of the initial and final states on the shock, $(\varepsilon^+, \sigma^+)$ and $(\varepsilon^-, \sigma^-)$. However, the question of the strain-stress path arises naturally if we take into account that a real shock in the soil is continuous, has a nonzero thickness and, if modelled within the framework of continuum mechanics, must have a definite strain-stress path. This path can be identified even for an idealised zero-thickness shock with the help of the energy balance.

For the analysis of shock propagation we have used two conservation laws (1), (3) for two unknown functions σ, ε, which yields two jump conditions (24). Given σ^+, σ^-, v^+ and a function $\sigma^-(\varepsilon)$, the two jump conditions enable us to determine the shock, i.e. to find two unknowns v^-, s. The energy balance is another conservation law which has not been used so far. For the present one-dimensional case, the energy balance can be written either in the integral form

$$\frac{d}{dt}\int_{x_a}^{x_b}\left(E+\frac{1}{2}\varrho v^2\right)dx-(\sigma v)\Big|_{x_a}^{x_b}=0 \tag{26}$$

or in the differential form

$$\frac{\partial}{\partial t}\left(E+\frac{1}{2}\varrho v^2\right)-\frac{\partial}{\partial x}(\sigma v)=0, \tag{27}$$

where E is the internal energy of the medium per unit volume. For continuous solutions, the energy balance (27) together with the equation of motion (1) and the kinematic relation (3) leads to the familiar expression for the energy rate:

$$\frac{\partial E}{\partial t}=\sigma\frac{\partial \varepsilon}{\partial t}. \tag{28}$$

For discontinuous solutions, the conservation law (27) yields the jump condition

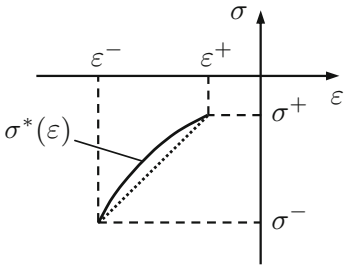

Fig. 12. Strain-stress path on the shock

$$\left[\!\left[E + \frac{1}{2}\varrho v^2\right]\!\right] s = -[\![\sigma v]\!]. \tag{29}$$

Using (29), (24) and the formulae for the jump of a product,

$$[\![ab]\!] = [\![a]\!]b^+ + [\![b]\!]a^- = \frac{1}{2}(b^+ + b^-)[\![a]\!] + \frac{1}{2}(a^+ + a^-)[\![b]\!], \tag{30}$$

we can derive an expression for the jump in the internal energy:

$$[\![E]\!] = \frac{1}{2}(\sigma^+ + \sigma^-)[\![\varepsilon]\!]. \tag{31}$$

If the deformation path on the shock is described by some function $\sigma^*(\varepsilon)$, then, according to (28), the increase in the internal energy across the shock is

$$\Delta E^{(1)} = \int_{\varepsilon^+}^{\varepsilon^-} \sigma^*(\varepsilon) d\varepsilon > 0. \tag{32}$$

On the other hand, the increase in the internal energy across the shock is $\Delta E^{(2)} = -[\![E]\!] > 0$. As follows from the comparison of (31) and (32), for any curve $\sigma^*(\varepsilon)$ that lies above the linear path (Fig. 12),

$$\Delta E^{(1)} < \Delta E^{(2)}, \tag{33}$$

and the energy balance is violated. Hence, the strain-stress path across the shock must be linear independently of the form of the function $\sigma^-(\varepsilon)$ between ε^+ and ε^-. This seeming discrepancy is resolved in the next Section where we consider smooth shocks of nonzero thickness.

6 Viscous Shocks

Smooth shocks can be obtained by introducing an additional viscous stress $\sigma_{vis} = \mu\, \partial v/\partial x$, where μ is a viscosity coefficient. The equation of motion (1) then becomes

$$\frac{\partial \sigma}{\partial x} + \frac{\partial \sigma_{vis}}{\partial x} = \varrho \frac{\partial v}{\partial t}, \tag{34}$$

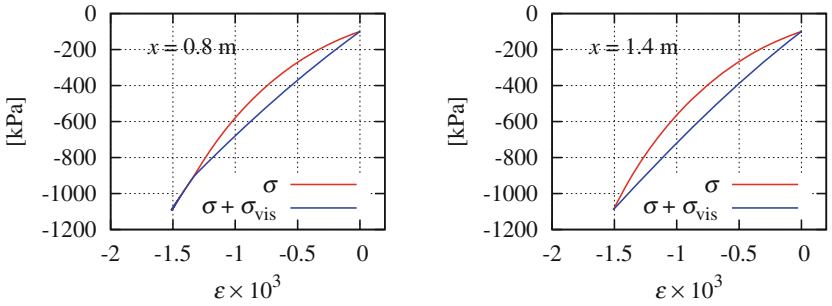

Fig. 13. Stresses as functions of the strain at two points in the numerical solution shown in Fig. 3

where σ is the rate-independent constitutive stress determined by a function $\sigma(\varepsilon)$. This approach has been used for the numerical solution of the boundary value problem for the half-space formulated in Sect. 2. The stress σ is given by the constitutive model (16) with the parameters from Table 1. The solution for dry soil shown in Fig. 3 is obtained by the finite-difference method with the viscosity coefficient $\mu = 10^{-3}\,\mathrm{MPa}\cdot\mathrm{s}$ and 1300 discretization points between $x = 0$ and $x = 1.8\,\mathrm{m}$.

As can be inferred from Fig. 3, the wave front that passes, for instance, through the point $x = 0.8\,\mathrm{m}$ has not yet fully turned into a shock and has both a (theoretically) discontinuous part from $\sigma^+ = -100\,\mathrm{kPa}$ to $\sigma^- = -900\,\mathrm{kPa}$ and a continuous part from -900 to $-1100\,\mathrm{kPa}$. The front that passes through the point $x = 1.4\,\mathrm{m}$ is entirely discontinuous from $\sigma^+ = -100\,\mathrm{kPa}$ to $\sigma^- = -1100\,\mathrm{kPa}$. Figure 13 shows the stresses as functions of the strain at these two points. While the stress σ follows the curve determined by the constitutive equation, the total stress $\sigma + \sigma_{vis}$ follows a linear strain-stress path on the discontinuous part of the front. The viscous stress on the shock develops to such an extent that the total stress becomes a linear function of the strain, and the energy balance (31), (32) is satisfied. Given σ^+ and σ^-, the viscous stress on the shock is the difference between the linear function and the constitutive curve $\sigma(\varepsilon)$ and, therefore, does not depend on the viscosity coefficient μ. The value of μ determines the shock thickness: the greater μ, the thicker the shock. The discontinuous shock is obtained as a limit for $\mu \to 0$ with the same viscous stress and the linear strain-stress relation on the shock.

As the numerical viscous shock shown in Fig. 3 propagates, it tends to a travelling-wave solution (a steady shock). The problem of finding this asymptotic solution is formulated as follows: given σ^+, σ^-, v^+, find the wave speed c and the functions $\varepsilon(y), v(y)$, where $y = x - ct$, $y \in (-\infty, +\infty)$, which satisfy (3), (34) and the boundary conditions

$$\lim_{y\to+\infty} \sigma(y) = \sigma^+, \qquad \lim_{y\to-\infty} \sigma(y) = \sigma^-, \qquad \lim_{y\to+\infty} v(y) = v^+, \tag{35}$$

$$\lim_{y\to+\infty} \sigma_{vis}(y) = 0, \qquad \lim_{y\to-\infty} \sigma_{vis}(y) = 0. \tag{36}$$

The constitutive function $\sigma(\varepsilon)$ is assumed to be such that $d^2\sigma/d\varepsilon^2 < 0$. The solution to this problem can be derived in explicit form. For brevity, we omit intermediate computations and present the final result. It can be verified directly that the solution satisfies the equations and the boundary conditions. In the formulae below, ε^+ and ε^- are determined from the constitutive function: $\sigma(\varepsilon^+) = \sigma^+, \sigma(\varepsilon^-) = \sigma^-$.

The speed of the smooth viscous shock is the same as that of a discontinuous shock:

$$c^2 = \frac{\sigma^+ - \sigma^-}{\varrho(\varepsilon^+ - \varepsilon^-)}. \tag{37}$$

The inverse to the function $\varepsilon(y)$ is given by the integral

$$y(\varepsilon) = \mu c \int_{\varepsilon_0}^{\varepsilon} \frac{d\eta}{\sigma(\eta) - \sigma^- - \varrho c^2(\eta - \varepsilon^-)}, \tag{38}$$

where $\varepsilon \in (\varepsilon^-, \varepsilon^+)$, and ε_0 is an arbitrary fixed strain between ε^- and ε^+. The velocity profile is obtained from the function $\varepsilon(y)$:

$$v(y) = -c\varepsilon(y) + c\varepsilon^+ + v^+. \tag{39}$$

This gives the unknown quantity $v^- = \lim_{y\to-\infty} v(y)$:

$$v^- = -c\varepsilon^- + c\varepsilon^+ + v^+. \tag{40}$$

Equation (40) coincides with the second jump condition (24). The first jump condition (24) also holds true and can readily be derived from (37) and (40). As we have seen in Sect. 2, the strain-stress relation in a travelling wave is necessarily linear. In the present case, this relation is

$$\sigma(y) + \sigma_{vis}(y) = \frac{\sigma^+ - \sigma^-}{\varepsilon^+ - \varepsilon^-}\left(\varepsilon(y) - \varepsilon^+\right) + \sigma^+. \tag{41}$$

7 Concluding Remarks

The strain-stress relation for soil in compression is nonlinear with increasing stiffness. This nonlinearity strongly influences the propagation of compression waves: a smooth wave front steepens and turns into a shock front. If the constitutive behaviour is rate-independent, the solution becomes discontinuous. The distance covered by a smooth front before it becomes discontinuous (the critical distance) is determined by (13). The critical distance depends on the stress rate applied at the boundary and on the curvature of the strain-stress function. For given medium and boundary loading, the critical distances for the cylindrical and spherical waves are related to the critical distance for the plane wave by (14), (15). The relations are independent of the constitutive function. The propagation of waves with discontinuities is governed, besides the differential equations for the smooth part of the wave, by the jump conditions (24) on the shock fronts. The same jump conditions hold true for steady viscous shocks.

The soil deformation on the shock is essentially different from the deformation on the smooth part of the wave. The strain rate on the shock is not only high but also highly inhomogeneous in space, Fig. 11. Using the same strain-stress curve for the shock and for the smooth part of the wave should be regarded as approximation.

References

1. Courant, R., Friedrichs, K.O.: Supersonic Flow and Shock Waves. Springer, New York (1976)
2. LeVeque, R.J.: Numerical Methods for Conservation Laws. Birkhäuser, Basel (1992)
3. Chorin, A.J., Marsden, J.E.: A Mathematical Introduction to Fluid Mechanics. Springer, New York (1993)
4. Smoller, J.: Shock Waves and Reaction-Diffusion Equations. Springer, New York (1994)
5. Toro, E.F.: Riemann Solvers and Numerical Methods for Fluid Dynamics: A Practical Introduction. Springer, Berlin (2009)
6. Courant, R., Hilbert, D.: Methods of Mathematical Physics: Partial Differential Equations, vol. 2. Interscience Publishers, New York (1965)
7. Osinov, V.A.: On the formation of discontinuities of wave fronts in a saturated granular body. Continuum Mech. Thermodyn. **10**(5), 253–268 (1998)
8. Osinov, V.A.: Critical distances for the formation of strong discontinuities in fluid-saturated solids. Arch. Appl. Mech. **80**, 581–592 (2010)
9. Osinov, V.A.: Transition from acceleration waves to strong discontinuities in fluid-saturated solids: drained versus undrained behaviour. Acta Mech. **211**, 181–193 (2010)
10. Lambe, T.W., Whitman, R.V.: Soil Mechanics. Wiley, New York (1969)
11. Richart, F.E., Hall, J.R., Woods, R.D.: Vibrations of Soils and Foundations. Prentice-Hall, Englewood Cliffs (1970)
12. Santamarina, J.C., Klein, K.A., Fam, M.A.: Soils and Waves. Wiley, Chichester (2001)
13. Osinov, V.A.: Blast-induced waves in soil around a tunnel. Arch. Appl. Mech. **81**, 543–559 (2011)
14. Osinov, V.A., Chrisopoulos, S., Triantafyllidis, Th.: Numerical analysis of the tunnel-soil interaction caused by an explosion in the tunnel. Soil Dyn. Earthq. Eng. **122**, 318–326 (2019)
15. Osinov, V.A., Chrisopoulos, S.: Two neighbouring tunnels in saturated soil under blast loading. This volume
16. Lax, P.D.: Hyperbolic Systems of Conservation Laws and the Mathematical Theory of Shock Waves. SIAM, Philadelphia (1973)
17. Lax, P.D.: Hyperbolic Partial Differential Equations. Courant Institute of Mathematical Sciences, New York (2006)
18. Trangenstein, J.A.: Numerical Solution of Hyperbolic Partial Differential Equations. Cambridge University Press, Cambridge (2007)